Available online at www.sciencedirect.com
SCIENCE DIRECT®
Journal of Sound and Vibration 283 (2005) 543–560
JOURNAL OF SOUND AND VIBRATION
www.elsevier.com/locate/jsvi

The controlling mechanism and the controlling effectiveness of passive mega-sub-controlled frame subjected to random wind loads

Zhang Xun'an[a,*], Wang Dong[a], Jiang Jiesheng[b]

[a]*Department of Civil Engineering, Northwestern Polytechnical University, Xian 710072, People's Republic of China*
[b]*Institute of Vibration Engineering, Northwestern Polytechnical University, Xian 710072, People's Republic of China*

Received 30 June 2003; received in revised form 13 April 2004; accepted 28 April 2004
Available online 11 November 2004

Abstract

The passive mega-sub-controlled structure proposed recently is a new form of structures associated with the design and construction of super tall buildings. However, as the dynamic characteristics of a practical passive mega-sub-controlled structure are very complicated, it is difficult to further all-sidedly examine the performance and the controlling effectiveness of this structure by a simple analytical model. In this paper, a new practical steel passive mega-sub-controlled frame is designed with reference to the conventional mega-sub-frame used in Tokyo City Hall. A more realistic analytical model of this structure subjected to random wind loads in which a non-white stochastic process in time and space is used is presented, and the coherence of the wind loads is further considered. The dynamic equations and the response spectrum expressions as well as the mean square response expressions are derived based on complex modal analysis theory. Moreover, the relative mass ratio RM and the relative stiffness ratio RD between the megaframe and the substructures are defined. The controlling effectiveness with different RM and RD is investigated. The results show that there exist some different controlling mechanisms, which are for the first time detected in this paper. As RD is less than certain value, $RD < 0.477$ for this building, the first vibration mode or the first–second vibration modes can be suppressed, and a remarkable controlling effectiveness can be obtained. However, as RD is greater than this value, the first vibration mode cannot be suppressed; the controlling effectiveness is unacceptable and is not like the expectations reported in earlier references.

*Corresponding author.
E-mail address: jiaoping@nwpu.edu.cn (Z. Xun'an).

0022-460X/$ - see front matter © 2004 Elsevier Ltd. All rights reserved.
doi:10.1016/j.jsv.2004.04.038

1. Introduction

The most significant engineering concerns in construction of tall buildings and super tall buildings are the safety of building structures and the comfort of occupants under external forces such as winds and earthquakes. For buildings with modest height, implementation of passive control devices offers a potential improvement in structural safety, performance of non-structural component, and human comfort, as these devices alter the dynamic characteristics of the structures to reduce structural response to external loads. For example, tuned mass damper systems have been applied to several buildings and were found to be effective in suppressing wind vibration. It is difficult, however, to introduce the conventional tuned mass damper system in tall or super tall buildings, since a heavier additional mass is required and a longer stroke must be accommodated in this case, thus raising significant safety concerns. Adding damping devices to the structure is another way to reduce the building vibration. Unfortunately, the structural characteristics common to most tall and super tall buildings, such as high shear rigidity and dominant bending deformation, tend to prevent the application of conventional damping devices.

A new method for controlling the response of tall buildings or super tall buildings under severe external loads was first introduced by Feng and Mita [1]. This method takes advantage of the so-called mega-sub-structural configuration which is gaining popularity in design and construction of tall and super tall buildings, e.g., the Bank of China at Hong Kong and Tokyo City Hall at Japan. A mega-sub-building consists of two major components—a megastructure which is the main structural frame of the building and several substructures each of which may contain several floors used for residential and/or commercial purposes. In conventional design, compared to the design proposed, these substructures are fixedly connected with the megastructure. The new mega-sub-structure named as passive mega-sub-controlled structure, proposed by Feng and Mita, exhibits isolated substructures, and these substructures can be used to suppress the vibration of the entire building. The function of these substructures is similar to that of the conventional tuned mass damper system in principle. This proposed structure, however, is more advantageous than the conventional tuned mass damper system. First of all, no additional mass is needed and the safety concern associated with the tuned mass damper device for tall and super tall buildings is eliminated. Second and more important, the mass ratio between the sub- and mega-structures is much higher (as high as 100%) than that in the tuned mass damper system (usually 1%). It is this feature that makes the proposed control method much more effective.

In an earlier study, Feng and Mita [1] performed preliminary investigation under the assumption that the wind load was a white noise and the building was modeled as a shear structure. Later, Chai and Feng [2] improved this analytical model, using a cantilever beam to represent the megastructure and a concentrated mass to represent the substructure. The time-histories analysis of this structure was investigated, in which a non-white noise stochastic process was employed to compute the wind loads. Recently, Lan Zhongjian et al. [3] proposed a multifunction mega-sub-controlled structure, which has the function of the mass dampers and base isolates as well as damping energy dissipation. The elastic–plastic time-histories analysis and the test of a simple building model were made. However, these analyses were based on the assumption that each substructure, which is the multi-degree-of-system freedom (mdof), was treated as only one concentrated mass, and the coherence of the wind loads was not considered. Therefore, the results could not explain some confused phenomena; e.g., in some case the practical

passive mega-sub-controlled structure will not have a good controlling behavior. Moreover, by the time-histories analytical method it is difficult to investigate these phenomena.

In this paper, a more realistic analytical model for this structure is proposed, and a practical steel passive mega-sub-controlled frame is investigated, which is designed with reference to the conventional mega-sub-frame of Tokyo City Hall. The corresponding dynamic equations are obtained under random wind loads, in which the Davenport wind speed spectrum is used, and the coherence of the wind loads is taken into account. It is found, however, that these equations cannot be decoupled, even if the damping matrices of the megaframe and the substructures are classical. Therefore the complex modal analytical theory of random vibration is employed, and the expressions of the response spectrum and mean square response are derived. The controlling effectiveness of this structure with different relative mass and relative stiffness between the megaframe and the substructure is examined, and the different controlling mechanisms are detected, which have not been reported in other papers, within our best knowledge up to now.

2. The analytical model of the passive mega-sub-controlled frame

The configuration of a conventional mega-sub-frame system is illustrated in Fig. 1, where the main structure is the megaframe, composed of megacolumns and megabeams with several subframes attached. Usually each subframe is connected with the megacolumns and megabeams, and contains 10–12 floors of steel megaframe or 4–6 floors of reinforced concrete megaframe [6]. As pointed out earlier, each subframe can be designed as an isolated substructure, that is carried by megabeams, as shown in Fig. 2. These proposed substructures should enable that the interaction between the megaframe and substructures can be used to control or suppress the building vibration.

For a tall or super tall building of this type, presented in Fig. 2, the bending is the dominant vibration mode for megaframe, which can be modeled as a mdof system, and the shearing is the governing mode for the substructures, since the substructures are usually not slender, (here it would be noticed that each substructure is also treated as a mdof system). Therefore, the analytical model of the passive mega-sub-controlled frame can be obtained as shown in Fig. 3, together with the conventional mega-sub-frame.

In Fig. 3, the passive mega-sub-controlled frame has n megafloors and n_1 substructures each of which consists of n_z floors. Its dynamic equation can be expressed as

$$M\ddot{X} + C\dot{X} + KX = F(t), \tag{1}$$

where $X = [x_p^{\mathrm{T}}, x_1^{\mathrm{T}}, x_2^{\mathrm{T}}, \ldots, x_{n_1}^{\mathrm{T}}]^{\mathrm{T}}$ is the total deformation vector of the building with $n + n_1 n_z$ variables, and $x_p^{\mathrm{T}} = [x_{p,1}, x_{p,2}, \ldots, x_{p,n}]^{\mathrm{T}}$, $x_i^{\mathrm{T}} = [x_{i,1}, x_{i,2}, \ldots, x_{i,n_z}]^{\mathrm{T}}$ $(i = 1, 2, \ldots, n_1)$ are deformation vectors of megaframe and ith substructure, respectively. $F(t) = [f(z,t)_p^{\mathrm{T}}, 0^{\mathrm{T}}]^{\mathrm{T}}$ is the load vector, and $f(z,t)_p^{\mathrm{T}} = [f(1,t)_p, f(2,t)_p, \ldots, f(n,t)_p]^{\mathrm{T}}$ is the random wind load vector forced on the megaframe.

- The expression of mass matrix

The mass matrix M in Eq. (1) can be expressed as

$$M = \mathrm{diag}[M_p, M_1, M_2, \ldots M_i \ldots, M_{n_1}], \tag{2}$$

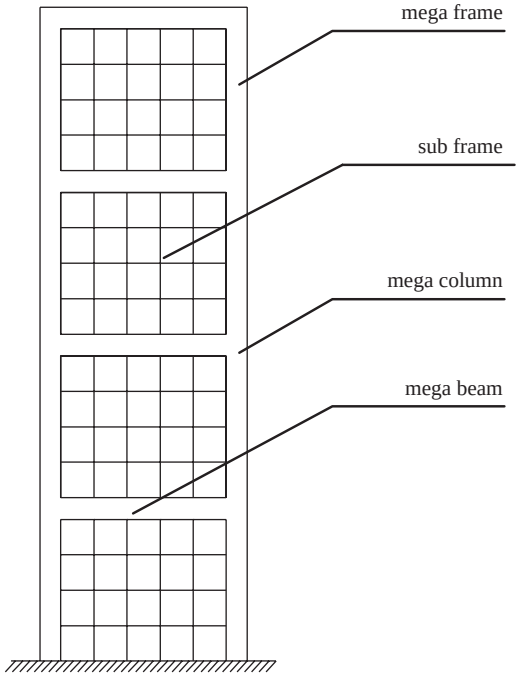

Fig. 1. The conventional mega-sub-frame.

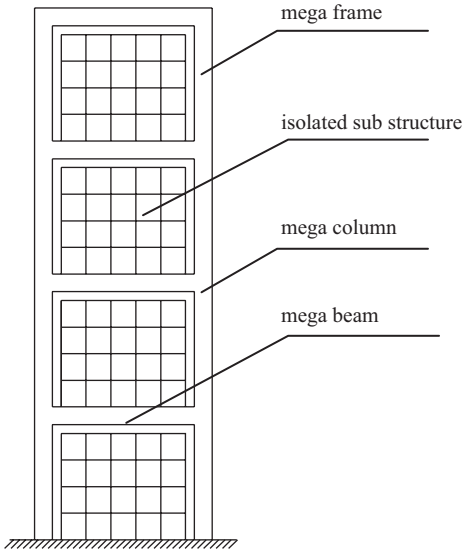

Fig. 2. The passive mega-sub-controlled frame.

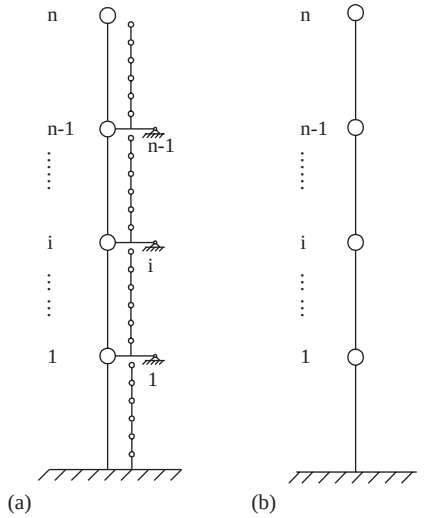

Fig. 3. (a) The analytical model of the passive mega-sub-controlled frame; (b) the analytical model of the conventional mega-sub-frame.

where M_p is $n \times n$ diagonal mass matrix of the megaframe, and M_i $(i = 1, 2, \ldots, n_1)$ is the $n_z \times n_z$ diagonal mass matrix of the ith substructure.

- The expression of stiffness matrix

The stiffness matrix in Eq. (1) can be written as

$$K = \begin{bmatrix} K_p + K_{s,\mathrm{diag}} & K_c \\ K_c^{\mathrm{T}} & K_s \end{bmatrix}, \quad K_s = \mathrm{diag}[K_{s1}, K_{s2}, \ldots, K_{si}, \ldots, K_{sn_1}], \tag{3}$$

where K_p is the $n \times n$ stiffness matrix of the megaframe, K_{si} $(i = 1, 2, \ldots, n_1)$ is the $n_z \times n_z$ stiffness matrix of the ith substructure, and $K_{s,\mathrm{diag}}$ has the following form:

$$K_{s,\mathrm{diag}} = \mathrm{diag}[k_{1,1}, k_{2,1}, \ldots, k_{i,1}, \ldots k_{n_1,1}, 0], \tag{4}$$

where $k_{i,1}$ $(i = 1, 2, \ldots, n_1)$ is the first floor shear stiffness value of the ith substructure. The matrix K_c in expression (3) is the coupling item between the megaframe and the substructures and has $n \times n_1 n_z$ matrix elements. Its non-zero elements can be expressed as

$$K_c(i,j) = -k_{i,1}, \quad j = (i-1)n_z + 1, \quad i = 1, 2, \ldots, n_1. \tag{5}$$

- The expression of damping matrix

The damping matrix C in Eq. (1) can be expressed as

$$C = \begin{bmatrix} C_p + C_{s,\mathrm{diag}} & C_c \\ C_c^{\mathrm{T}} & C_s \end{bmatrix}, \quad C_s = \mathrm{diag}[C_{s1}, C_{s2}, \ldots, C_{si}, \ldots, C_{sn_1}], \tag{6}$$

where C_p is the $n \times n$ damping matrix of the megaframe, and C_{si} $(i = 1, 2, \ldots, n_1)$ is the $n_z \times n_z$ damping matrix of the ith substructure.

The $n \times n_1 n_z$ matrix C_c in expression (6) is the coupling damping matrix between the megaframe and the substructures. Its non-zero elements are expressed as

$$C_c(i,j) = -c_{i,1}, \quad j = (i-1)n_z + 1, \quad i = 1, 2, \ldots, n_1, \tag{7}$$

where $c_{i,1}$ is the first floor damping value of the ith substructure. Finally the matrix $C_{s,\mathrm{diag}}$ in expression (6) can be presented as

$$C_{s,\mathrm{diag}} = \mathrm{diag}[c_{1,1}, c_{2,1}, \ldots, c_{i,1}, \ldots, c_{n_1,1}, 0]. \tag{8}$$

The details of assemblies for matrices K and C can be found in Appendix A.

3. The expressions of the response spectrum and mean square response

In order to analyze the controlling properties of the passive mega-sub-controlled frame, the dynamic equation (1) must be decoupled. For the sake of convenience, the real modal analytical method should be used. However, it is unfortunately found that, through the numerical computing check, Eq. (1) with the matrix C presented by expression (6) cannot be decoupled, as the following necessary decoupling and sufficient condition [4] is not met:

$$CM^{-1}K = KM^{-1}C. \tag{9}$$

Therefore, the complex modal analytical theory must be employed.

Defining the state vector $r = [\dot{X}^{\mathrm{T}}, X^{\mathrm{T}}]^{\mathrm{T}}$ and introducing this state vector into Eq. (1), the system eigenvalue p_i, and the left eigenvector v_i, as well as the right eigenvector u_i ($i = 1, 2, \ldots, 2 \times N$, and $N = n + n_1 \times n_z$) can been obtained [4]. By further making complex modal transformation, the decoupled dynamic equations of Eq. (1) can be expressed in the following form, as the orthogonality of the left and the right modal matrices is considered:

$$\dot{Z}_i - p_i \cdot Z_i = m_i'^{-1} v_i^{\mathrm{T}} F(t), \quad i = 1, 2, \ldots, 2N, \tag{10}$$

where Z_i is the ith complex modal coordinate and $m_i' = v_i^{\mathrm{T}}[2p_i M + C] \cdot u_i$.

By Duhamel integration, the response of Eq. (10) can be expressed as

$$Z_i(t) = \int_{-\infty}^{\infty} h_i(t-\mu) m_i'^{-1} v_i^{\mathrm{T}} F(\mu)\, \mathrm{d}\mu, \quad i = 1, 2, \ldots, 2N \tag{11}$$

and the cross-covariance function of the response $Z_i(t)$ and $Z_j(t)$ can be obtained from

$$E[Z_i(t_1)\bar{Z}_j^{\mathrm{T}}(t_2)] = \int_{-\infty}^{\infty} H_i(-\omega) m_i'^{-1} v_i^{\mathrm{T}} [S_{F_K F_L}(\omega)] \bar{v}_j \bar{m}_i'^{-1} \bar{H}_j^{\mathrm{T}}(-\omega) \mathrm{e}^{\mathrm{j}\omega(t_1 - t_2)}\, \mathrm{d}\omega, \tag{12}$$

where $H_i(-\omega)$ and $\bar{H}_j(-\omega)$ are, respectively, the ith modal frequency function and jth modal conjugate frequency function with $-\omega$, and have the following forms:

$$H_i(-\omega) = -\int_{-\infty}^{\infty} h_i(t_1 - \mu_1) \mathrm{e}^{\mathrm{j}\omega(t_1 - \mu_1)}\, \mathrm{d}\mu_1, \tag{13}$$

$$\bar{H}_j(-\omega) = -\int_{-\infty}^{\infty} \bar{h}_j(t_2-\mu_2)\mathrm{e}^{-\mathrm{j}\omega(t_2-\mu_2)}\,\mathrm{d}\mu_2. \tag{14}$$

The matrix $[S_{F_K F_L}(\omega)]$ in expression (12) denotes the cross-power spectrum matrix of turbulent wind loads; its element $S_{F_K F_L}(\omega)$ is computed according to the Davenport wind speed spectrum, which was derived in Ref. [5]:

$$S_{F_K F_L}(\omega) = \rho_{KL} F_K^* F_L^* S_f(\omega), \quad K, L = 1, 2, \ldots, n, \tag{15}$$

where ρ_{KL} is the coherence function in vertical direction between the kth mass and lth mass, and $S_f(\omega)$ is the power spectrum of turbulent wind pressure with the following form:

$$S_f(\omega) = \frac{2x^2}{3\omega(1+x^2)^{4/3}}, \quad x = \frac{30}{\sqrt{w_0}T_1}, \tag{16}$$

where w_0 is the mean wind pressure at 10 m height above the ground and T_1 is the turbulent wind period.

In expression (15) F_K^* exhibits the following form:

$$F_K^* = \frac{1}{\mu}\mu_{\cdot f}\mu_s \cdot \mu_y \cdot w_0 \cdot A_K, \quad K = 1, 2, \ldots, n, \tag{17}$$

where A_k is the tributary area of the kth mass in the wind direction, μ_f is the fluctuating coefficient, μ_s is the building body-type coefficient, μ_y is the wind profile coefficient in vertical direction and μ is the peak factor of turbulent wind.

From expression (12) the response power spectrum $S_{Z_i Z_j}(\omega)$ can be obtained by Fourier transformation:

$$S_{Z_i Z_j}(\omega) = H_i(-\omega)m_i'^{-1}v_i^{\mathrm{T}}[S_{F_K F_L}(\omega)]\bar{v}_j\bar{m}_i'^{-\mathrm{T}}\bar{H}_j^{\mathrm{T}}(-\omega), \quad i,j = 1, 2, \ldots, 2N, \quad K, L = 1, 2, \ldots, n. \tag{18}$$

By further considering the expression of the modal transformation, the response power spectrum matrix $S_r(\omega)$ in state space can be expressed as

$$S_r(\omega) = U[S_{Z_i Z_j}(\omega)]\bar{U}^{\mathrm{T}}, \tag{19}$$

where U is the right modal matrix.

Finally, the mean-square response of the passive mega-sub-controlled frame can be obtained from

$$\sigma^2 = \int_{-\infty}^{\infty} S_r(\omega)\,\mathrm{d}\omega. \tag{20}$$

For expression (20) the numerical integral method will be adopted.

4. The computing studies of a steel passive mega-sub-controlled frame

To investigate the performance of the passive mega-sub-controlled structure, a steel passive mega-sub-controlled frame is designed, as shown in Fig. 4a, with reference to the conventional

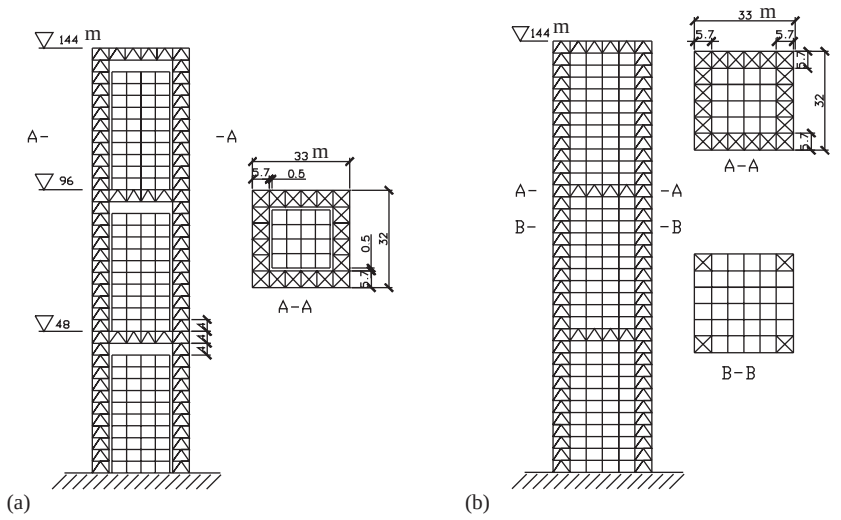

Fig. 4. The structures of (a) the new steel passive mega-sub-controlled frame and (b) the conventional mega-sub-frame used in Tokyo City Hall.

mega-sub-frame used in Tokyo City Hall presented in Fig. 4b. The two buildings have the same megaframe form: they are composed of latticed megacolumns and latticed megabeams, and are 144 m high with three megafloors. The cross sections of the latticed megacolumn and the latticed megabeam are $5.7\,\mathrm{m} \times 5.7\,\mathrm{m}$ and $5.7\,\mathrm{m} \times 4.0\,\mathrm{m}$, respectively. In Fig. 4a the passive mega-sub-controlled structure contains three isolated substructures; each substructure is 10 floors and each floor is 4 m high. In order to avoid collision between the megaframe and the isolated substructure under dynamic loads, a gap with 0.5 m width is designed between the megaframe and the isolated substructure, as shown in Fig. 4a.

The responses of these two buildings are numerically simulated and compared under random wind load. Here the two buildings have the same amount of total mass and same structural members as listed in Table 1, and have the same damping characteristics, which result in a 2% damping ratio. This 2% damping ratio is a typical value for tall steel buildings.

In order to further examine the controlling effectiveness of this passive mega-sub-controlled frame with different substructural mass and stiffness, the relative mass ratio RM and the relative stiffness ratio RD between the megaframe and the substructure are, respectively, defined as follows:

$$\mathrm{RM} = \frac{M_{\mathrm{sub}}}{M_{\mathrm{mega}}}, \quad \mathrm{RD} = \frac{K^*_{\mathrm{sub}}}{K^*_{\mathrm{mega}}},$$

where M_{mega} is the total mass of the megaframe, M_{sub} is the total mass of the substructure, K^*_{sub} is the shear stiffness of the substructure and K^*_{mega} is the bending stiffness of the megaframe. The calculations of K^*_{sub} and K^*_{mega} are described in Fig. 5. For the original design of this steel passive mega-sub-controlled frame the RM is 1.187, and the RD is 0.7633.

Table 1
The characteristic of the member sections

Member	The size of member section (mm)	A (cm^2)	I_x (cm^4)	I_y (cm^4)
The member of megacolumn in floor 1	□750 × 750 × 70 × 70	1904	1,482,899	1,482,899
The member of megacolumn in floor 2–12	□700 × 700 × 70 × 70	1764	1,181,292	1,181,292
The member of megacolumn in floor 13–24	□700 × 700 × 60 × 60	1535.6	1,057,400	1,057,400
The member of megacolumn in floor 25–36	□700 × 700 × 28 × 28	752.6	567450.4	567450.4
The member of megabeam in floor 11–12	H1000 × 450 × 28 × 36	583.8	939554.7	54844.76
The member of megabeam in floor 23–24	H1000 × 450 × 28 × 36	583.8	939554.7	54844.76
The member of megabeam in floor 35–36	H1000 × 350 × 16 × 28	347	575236.5	20040.6
The web member of megacolumn in floor 1–12	H350 × 350 × 25 × 25	250	51927.1	17903.7
The web member of megacolumn in floor 13–36	H350 × 350 × 12 × 19	170.4	39506.2	13581.6
The web member of megabeam in floor 12	H350 × 350 × 19 × 25	232	50577.1	17881.7
The web member of megabeam in floor 24	H350 × 350 × 19 × 25	232	50577.1	17881.7
The web member of megabeam in floor 36	H350 × 350 × 12 × 19	170.4	39506.2	13581.6
The member of subbeam	H1000 × 450 × 16 × 28	347	575236.5	20040.6
The member of subcolumn	H400 × 400 × 20 × 20	304	73,364	73,364
The secondary beam in megabeam	H1000 × 450 × 16 × 28	347	575236.5	20040.6

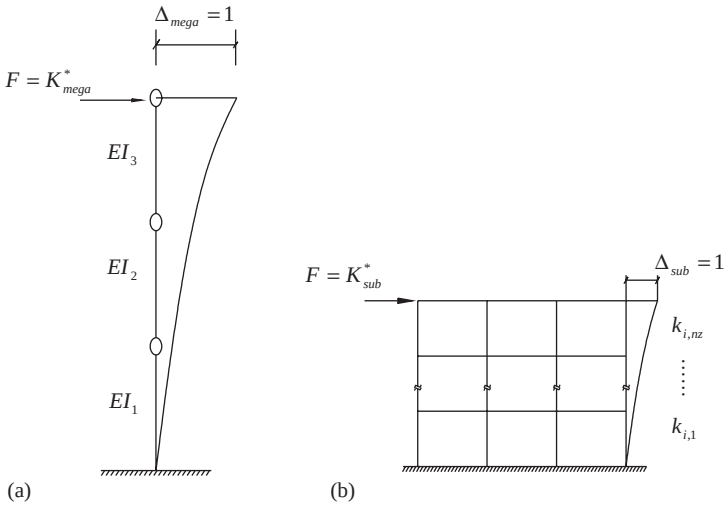

Fig 5. The calculations of (a) K^*_{mega} and (b) K^*_{sub} substructure where $k_{i,1}-k_{i,nz}$ is calculated by D-value method.

Fig. 6 presents the comparison of the response spectra at the top mass of the conventional mega-sub-frame and the top megamass of the passive mega-sub-controlled frame while RD = 0.7633 and RM = 1.187. It can be seen that in this situation the passive mega-sub-controlled

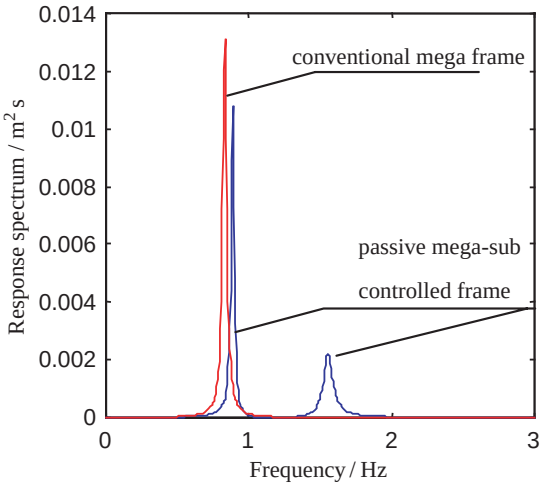

Fig. 6. The comparison of the response spectra at the top mass of the conventional mega-sub-frame and the top megamass of the passive mega-sub-controlled frame, while RD = 0.7633, RM = 1.187.

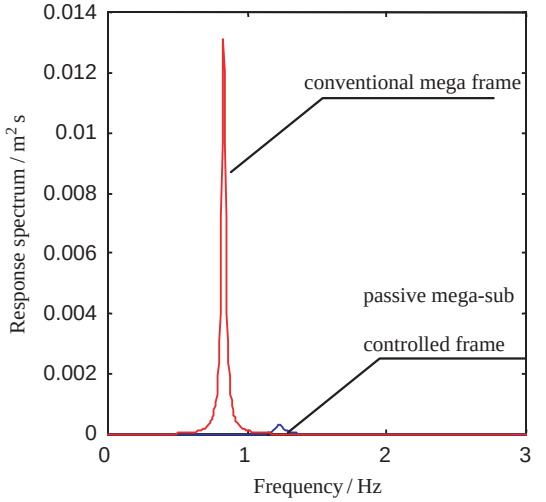

Fig. 7. The comparison of the response spectra at the top mass of the conventional mega-sub-frame and the top megamass of the passive mega-sub-controlled frame, while RD = 0.4771, RM = 1.187.

frame does not exhibit an expected well-behaved controlling effectiveness reported in other references, since the response spectrum is not improved obviously.

Fig. 7 presents the same comparison, while RD = 0.477 and RM = 1.187. In this case the response spectrum of the passive mega-sub-controlled frame is much less than that of the

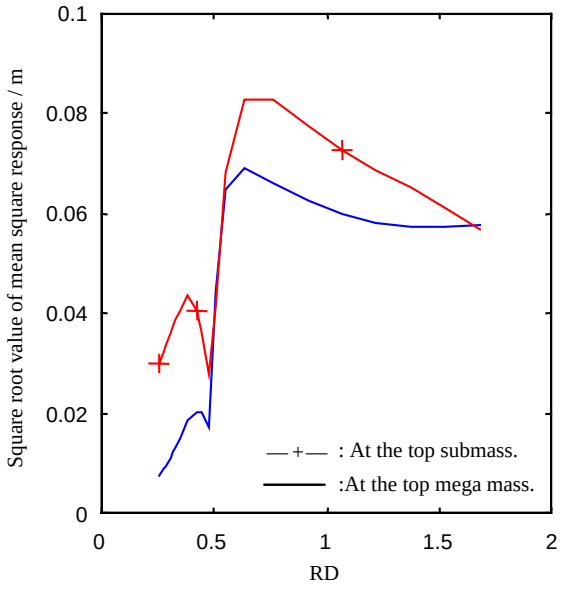

Fig. 8. The square root values of the mean square displacement responses of the passive mega-sub-controlled frame, while RM = 1.187 and RD = 0.25–1.55.

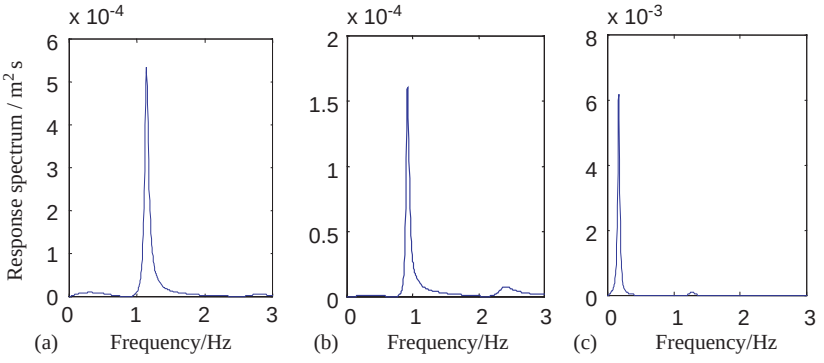

Fig. 9. Response spectra with different relative stiffness RD at the top megamass of the passive mega-sub-controlled frame: (a) RD = 0.427; the first–fourth natural frequencies of this system are 0.6265, 0.87474, 1.1366, 2.5995 Hz. (b) RD = 0.305; the first–fourth natural frequencies of this system are 0.73971, 0.91489, 1.1922, 2.1993 Hz. (c) RD = 0.511, and the first–fourth natural frequencies of this system are 0.16935, 0.95957, 1.2752, 2.8506 Hz.

conventional mega-sub-frame. It could be confirmed that, as RD = 0.477 and RM = 1.187, the passive mega-sub-controlled frame has an extraordinary controlling effectiveness.

Fig. 8 further presents the square root values of the mean square displacement responses at the top megamass and the top submass of the passive mega-sub-controlled frame as RD = 0.25–1.55 and RM = 1.187. It shows that, when RD is less than a certain value (RD $\leqslant$ 0.477), the responses of both the megaframe and the substructures are very little. However, while RD > 0.477, the responses will rise steeply and then tend to slightly decrease. These responses are generally

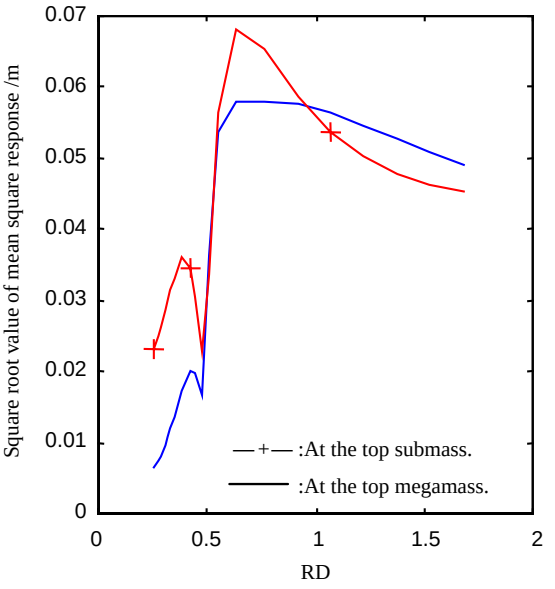

Fig. 10. The square root values of the mean square displacement responses of the passive mega-sub-controlled frame, while RM = 1.78 and RD = 0.25–1.55.

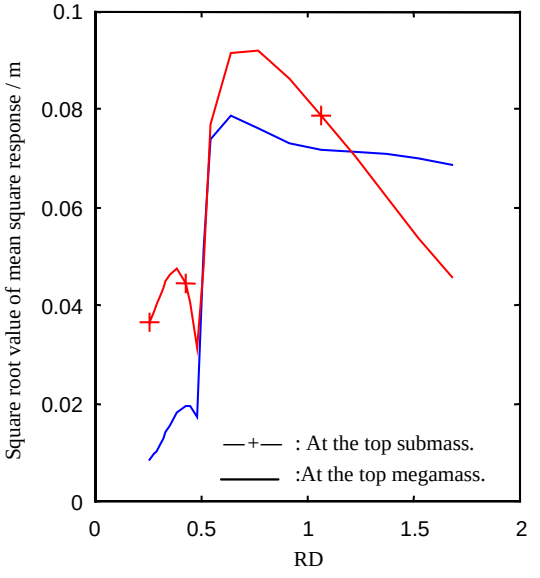

Fig. 11. The square root values of the mean square displacement responses of the passive mega-sub-controlled frame, while RM = 0.83 and RD = 0.25–1.55.

much greater than those responses in the range of RD $\leqslant$ 0.477. These clearly display that an effective controlling for both the megaframe and the substructures can be obtained while RD $\leqslant$ 0.477.

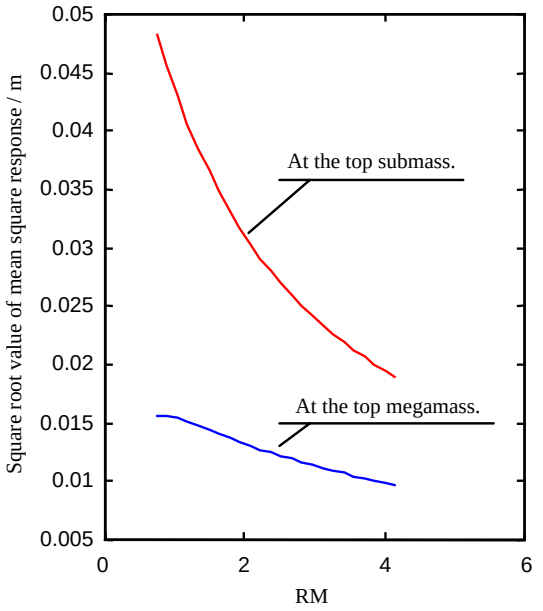

Fig. 12. The square root values of the mean square displacement responses of the passive mega-sub-controlled frame with different RM (0.6–4.15), while RD = 0.35.

The response spectra of this passive mega-sub-controlled frame are further investigated in detail; the results are shown in Fig. 9, which presents the response spectra at the top megamass. It is found that, while RD = 0.382–0.477, the response spectra are suppressed in the location of first and second natural frequency of the system, and mainly distributed at third natural frequency, as shown in Fig. 9(a). While RD < 0.382, the response spectra are chiefly located at second natural frequency, and also suppressed at first natural frequency, as shown in Fig. 9(b). However, it is contrary to these phenomena that, while RD > 0.477, the response spectra are seldom suppressed and chiefly distributed at first natural frequency as shown in Fig. 9(c).

When the relative mass ratio RM is added, the controlling effectiveness will be further improved. This can be explained by Fig. 10, which presents the square root values of the mean square displacement responses at the top megamass and the top submass of this structure as RM = 1.78 and RD = 0.25–1.55. However, as RM is decreased, these square root values will correspondingly increase, as shown in Fig. 11, where RM = 0.83 and RD = 0.25–1.55. Those variations of the controlling results with different relative mass ratio RM can be explained by Fig. 12, where the relative stiffness ratio RD is fixed on 0.35, and the relative mass ratio RM is varied from 0.35 to 4.12. It clearly shows that, as the relative mass ratio RM is increased, the responses at the top megamass and the top submass are decreased.

5. Conclusion

As the dynamic characteristics of a practical passive mega-sub-controlled frame are very complicated, it is necessary to further investigate its controlling mechanism and controlling

effectiveness based on a more realistic analytical model. In this paper, a practical steel passive mega-sub-controlled frame is investigated. The results show that the controlling effectiveness of this building with different relative stiffness ratio RD and different relative mass ratio RM is different. Especially, as RD is altered, some different controlling mechanisms are detected. While RD is less than some value, such as $\mathrm{RD} \leqslant 0.477$, a remarkable controlling effectiveness can be obtained based on the first or first–second vibration mode being suppressed. However, as RD is greater than this value, the first vibration mode cannot be suppressed, and the controlling effectiveness is unacceptable and is not like the expectations reported in earlier references, so that in practical engineering this phenomenon must be avoided.

Appendix A. The details of assemblies for matrices K and C

A.1. The stiffness matrix K

The submatrix $K_p + K_{s,\mathrm{diag}}$ in expression (3) can be assembled in the following form:

$$K_p + K_{s,\mathrm{diag}} =$$

$$\begin{array}{c} \\ 1 \\ 2 \\ \vdots \\ i \\ \vdots \\ n-1 \\ n \end{array}
\begin{array}{c}
\begin{array}{ccccccccc} 1 & & 2 & 3 & & i & & n-1 & n \end{array} \\
\left[\begin{array}{ccccccccc}
k_{p1,1}+k_{1,1} & & k_{p1,2} & k_{p1,3} & \cdots & k_{p1,i} & \cdots & k_{p1,n-1} & k_{p1,n} \\
k_{p2,1} & & k_{p2,2}+k_{2,1} & k_{p2,3} & \cdots & k_{p2,i} & \cdots & k_{p2,n-1} & k_{p2,n} \\
\vdots & & \vdots & \vdots & & \vdots & & \vdots & \vdots \\
k_{pi,1} & & k_{pi,2} & k_{pi,3} & \cdots & k_{pi,i}+k_{i,1} & \cdots & k_{pi,n-1} & k_{pi,n} \\
\vdots & & \vdots & \vdots & & \vdots & & \vdots & \vdots \\
k_{pn-1,1} & & k_{pn-1,2} & k_{pn-1,3} & \cdots & k_{pn-1,i} & \cdots & k_{pn-1,n-1}+k_{n_1,1} & k_{pn-1,n} \\
k_{pn,1} & & k_{pn,2} & k_{pn,3} & \cdots & k_{pn,i} & \cdots & k_{pn,n-1} & k_{pn,n}
\end{array}\right]_{n\times n}
\end{array}, \tag{A.1}$$

where $k_{pi,j}$ $(i,j = 1,2,3,\ldots,n)$ is the element of the stiffness matrix K_p of the megaframe, and $k_{i,1}$ $(i = 1,2,3,\ldots,n_1)$ is the first floor shear stiffness value of the ith substructure.

The submatrix K_c can be expressed in detail as

$$
K_c = \begin{array}{c}
\\
1 \\ 2 \\ 3 \\ \vdots \\ i \\ \vdots \\ n_1 \\ \vdots \\ n
\end{array}
\begin{bmatrix}
1 & 2 & \cdots & n_z{+}1 & n_z{+}2 & \cdots & 2n_z{+}1 & 2n_z{+}2 & \cdots & (i{-}1)n_z{+}1 \\
-k_{1,1} & 0 & \cdots & 0 & 0 & \cdots & 0 & 0 & \cdots & 0 \\
0 & 0 & \cdots & -k_{2,1} & 0 & \cdots & 0 & 0 & \cdots & 0 \\
0 & 0 & \cdots & 0 & 0 & \cdots & -k_{3,1} & 0 & \cdots & 0 \\
\vdots & \vdots & & \vdots & \vdots & & \vdots & \vdots & & \vdots \\
0 & 0 & \cdots & 0 & 0 & \cdots & 0 & 0 & \cdots & -k_{i,1} \\
\vdots & \vdots & & \vdots & \vdots & & \vdots & \vdots & & \vdots \\
0 & 0 & \cdots & 0 & 0 & \cdots & 0 & 0 & \cdots & 0 \\
\vdots & \vdots & & \vdots & \vdots & & \vdots & \vdots & & \vdots \\
0 & 0 & \cdots & 0 & 0 & \cdots & 0 & 0 & \cdots & 0
\end{bmatrix}
\begin{bmatrix}
(i{-}1)n_z{+}2 & & (n_1{-}1)n_z{+}1 & (n_1{-}1)n_z{+}2 & & n_1n_z \\
0 & \cdots & 0 & 0 & \cdots & 0 \\
0 & \cdots & 0 & 0 & \cdots & 0 \\
0 & \cdots & 0 & 0 & \cdots & 0 \\
\vdots & & \vdots & \vdots & & \vdots \\
0 & \cdots & 0 & 0 & \cdots & 0 \\
\vdots & & \vdots & \vdots & & \vdots \\
0 & \cdots & -k_{n_1,1} & 0 & \cdots & 0 \\
\vdots & & \vdots & \vdots & & \vdots \\
0 & \cdots & 0 & 0 & \cdots & 0
\end{bmatrix}_{n\times n_1n_2}
\tag{A.2}
$$

The submatrix K_s is composed of diagonal matrix K_{si}, as presented in expression (3), which can be expressed as

$$K_{si} = \begin{bmatrix} k_{i,1}+k_{i,2} & -k_{i,2} & 0 & 0 & \cdots & 0 \\ -k_{i,2} & k_{i,2}+k_{i,3} & -k_{i,3} & 0 & \cdots & 0 \\ & \ddots & \ddots & \ddots & & \\ 0 & 0 & \cdots & -k_{i,n_z-1} & k_{i,n_z-1}+k_{i,n_z} & -k_{i,n_z} \\ 0 & 0 & \cdots & 0 & -k_{i,n_z} & k_{i,n_z} \end{bmatrix}_{n_z \times n_z}, \tag{A.3}$$

where $k_{i,j}$ $(j = 1, 2, 3, \ldots, n_z)$ is the jth floor stiffness value of the ith substructure.

From the above expressions (A.1)–(A.3) and expression (3) we can conclude that the stiffness matrix K is a $(n + n_1 n_z) \times (n + n_1 n_z)$ matrix.

A.2. The damping matrix C

The assembly of damping matrix C in expression (6) is in the same way as the assembly of stiffness matrix K, i.e., the submatrix $C_p + C_{s,\mathrm{diag}}$ can be expressed as

$$C_p + C_{s,\mathrm{diag}} = \begin{array}{c} \\ 1 \\ 2 \\ \vdots \\ i \\ \vdots \\ n-1 \\ n \end{array} \begin{array}{c} \begin{array}{cccccccc} 1 & 2 & 3 & & i & & n-1 & n \end{array} \\ \begin{bmatrix} c_{p1,1}+c_{1,1} & c_{p1,2} & c_{p1,3} & \cdots & c_{p1,i} & \cdots & c_{p1,n-1} & c_{p1,n} \\ c_{p2,1} & c_{p2,2}+c_{2,1} & c_{p2,3} & \cdots & c_{p2,i} & \cdots & c_{p2,n-1} & c_{p2,n} \\ \vdots & \vdots & \vdots & & \vdots & & \vdots & \vdots \\ c_{pi,1} & c_{pi,2} & c_{pi,3} & \cdots & c_{pi,i}+c_{i,1} & \cdots & c_{pi,n-1} & c_{pi,n} \\ \vdots & \vdots & \vdots & & \vdots & & \vdots & \vdots \\ c_{pn-1,1} & c_{pn-1,2} & c_{pn-1,3} & \cdots & c_{pn-1,i} & \cdots & c_{pn-1,n-1}+c_{n_1,1} & c_{pn-1,n} \\ c_{pn,1} & c_{pn,2} & c_{pn,3} & \cdots & c_{pn,i} & \cdots & c_{pn,n-1} & c_{pn,n} \end{bmatrix}_{n \times n} \end{array}, \tag{A.4}$$

where $c_{pi,j}$ $(i, j = 1, 2, 3, \ldots, n)$ is the element of the damping matrix C_p of the megaframe, and the $c_{i,1}$ $(i = 1, 2, \ldots, n_1)$ is the first floor damping value of the ith substructure.

The submatrix C_c in expression (7) exhibits

$$
C_c = \begin{array}{c}
\\
1 \\
2 \\
3 \\
\vdots \\
i \\
\vdots \\
n_1 \\
\vdots \\
n
\end{array}
\begin{array}{c}
\begin{array}{cccccccccc}
1 & 2 & & n_z{+}1 & n_z{+}2 & & 2n_z{+}1 & 2n_z{+}2 & & (i{-}1)n_z{+}1
\end{array} \\
\left[\begin{array}{cccccccccc}
-c_{1,1} & 0 & \cdots & 0 & 0 & \cdots & 0 & 0 & \cdots & 0 \\
0 & 0 & \cdots & -c_{2,1} & 0 & \cdots & 0 & 0 & \cdots & 0 \\
0 & 0 & \cdots & 0 & 0 & \cdots & -c_{3,1} & 0 & \cdots & 0 \\
\vdots & \vdots & & \vdots & \vdots & & \vdots & \vdots & & \vdots \\
0 & 0 & \cdots & 0 & 0 & \cdots & 0 & 0 & \cdots & \\
\vdots & \vdots & & \vdots & \vdots & & \vdots & \vdots & -c_{i,1} & \vdots \\
0 & 0 & \cdots & 0 & 0 & \cdots & 0 & 0 & \cdots & 0 \\
\vdots & \vdots & & & \vdots & & \vdots & \vdots & & \vdots \\
0 & 0 & \cdots & 0 & 0 & \cdots & 0 & 0 & \cdots & 0
\end{array}\right.
\end{array}
$$

$$
\begin{array}{c}
\begin{array}{cccccc}
(i{-}1)n_z{+}2 & & (n_1{-}1)n_z{+}1 & (n_1{-}1)n_z{+}2 & & n_1n_z
\end{array} \\
\left.\begin{array}{cccccc}
0 & \cdots & 0 & 0 & \cdots & 0 \\
0 & \cdots & 0 & 0 & \cdots & 0 \\
0 & \cdots & 0 & 0 & \cdots & 0 \\
\vdots & & \vdots & \vdots & & \vdots \\
0 & \cdots & 0 & 0 & \cdots & 0 \\
\vdots & & \vdots & \vdots & & \vdots \\
0 & \cdots & -c_{n_1,1} & 0 & \cdots & 0 \\
\vdots & & \vdots & \vdots & & \vdots \\
0 & \cdots & 0 & 0 & \cdots & 0
\end{array}\right]_{n\times n_1n_2}
\end{array}
, \qquad \text{(A.5)}
$$

The submatrix C_{si} in expression (6) has the following form:

$$C_{si} = \begin{bmatrix} c_{i,1}+c_{i,2} & -c_{i,2} & 0 & 0 & \cdots & 0 \\ -c_{i,2} & c_{i,2}+c_{i,3} & -c_{i,3} & 0 & \cdots & 0 \\ & \ddots & \ddots & \ddots & & \\ 0 & 0 & \cdots & -c_{i,n_z-1} & c_{i,n_z-1}+c_{i,n_z} & -c_{i,n_z} \\ 0 & 0 & \cdots & 0 & -c_{i,n_z} & c_{i,n_z} \end{bmatrix}_{n_z \times n_z}, \tag{A.6}$$

where $c_{i,j}$ $(j = 1, 2, 3, \ldots, n_z)$ is the jth floor damping value of the ith substructure.

Finally, based on expressions (A.4)–(A.6) and expression (6), the damping matrix C, which is a $(n + n_1 n_z) \times (n + n_1 n_z)$ matrix, can be easily assembled.

References

[1] M.Q. Feng, A. Mita, Vibration control of tall buildings using mega-sub configuration, *Journal of Engineering Mechanics* 121 (10) (1995) 1082–1087.

[2] W. Chai, M.Q. Feng, Vibration control of super tall buildings subjected to wind loads, *International Journal of Nonlinear Mechanics* 32 (4) (1997) 657–668.

[3] Lan Zhongjian, Fang Liang, Wang Xinde, Multifunctional shock-absorption system of RC megaframe structures, *Industrial Construction* 32 (2) (2002) 1–4.

[4] T. Fang, *Engineering Random Vibration*, first ed, The Press of National Defense Industry, Beijing, 1995.

[5] Zhang Xun'an, Jiang Jiesheng, The random responses of internal force for tall TV towers under wind loads, *Journal of Northwestern Polytechnical University* 18 (5) (2000) 179–182.

[6] Zhou Xiaofeng, Dong Shilin, The dynamical analysis of the steel megaframe, *Building Structure* 31 (6) (2001) 3–9.